Chemical and Biological Technologies in Agriculture

RESEARCH

Open Access

Antifungal activity and application of *Bacillus tequilensis* A13 in biocontrol of *Rehmannia glutinosa* root-rot disease

Ruifei Wang[1,2], Haibing Li[1], Zhao Qin[1], Yan Wang[1], Qingxiang Yang[1,2*], Hao Zhang[1,2] and Mingjun Li[1,3]

Abstract

Background The bacterial genus *Bacillus*, an important group of bacteria which can suppress phytopathogens, has been widely used in agriculture. However, different species of *Bacillus* often displayed significant differences in probiotic efficiency and mechanism, suggesting that it is very necessary to investigate the biocontrol potential of new *Bacillus* isolates, especially from under-evaluated *Bacillus* spp. *Rehmannia glutinosa* (*R. glutinosa*), an important traditional Chinese medicinal herb, is affected by a serious root-rot disease caused by the fungus *Fusarium solani* (*F. solani*). Biocontrol agents against this root-rot disease in *R. glutinosa* have yet to be developed. This study explored, for the first time, the activity and biocontrol mechanism of a new *Bacillus* isolate, *Bacillus tequilensis* A13, in antagonizing *F. solani*.

Results *B. tequilensis* A13 displayed a strong inhibitory activity (73.49% ± 1.33%) against *F. solani* growth in vitro and was able to survive and multiply in the sterilized soil. The results from liquid chromatography electrospray ionization tandem mass spectrometry (LC–MS/MS) and Gene Ontology (GO) analyses indicated that *B. tequilensis* A13 cell-free supernatant contained six antifungal compounds, eight antifungal compound synthases, and several functional proteins involved in the processes of plant stress resistance, etc. Finally, the joint application of complex fertilizer together with *B. tequilensis* A13 significantly reduced the incidence of *R. glutinosa* root rot in the field.

Conclusion *B. tequilensis* A13 strongly inhibited *F. solani* growth by producing antifungal compounds and proteins associated with plant stress resistance/tolerance, and proved to be a promising candidate biocontrol agent against *R. glutinosa* root-rot disease.

Keywords Biocontrol, Root-rot disease, *Bacillus tequilensis*, *Fusarium solani*, *Rehmannia glutinosa*

*Correspondence:
Qingxiang Yang
yangqx@htu.edu.cn
Full list of author information is available at the end of the article

Graphical Abstract

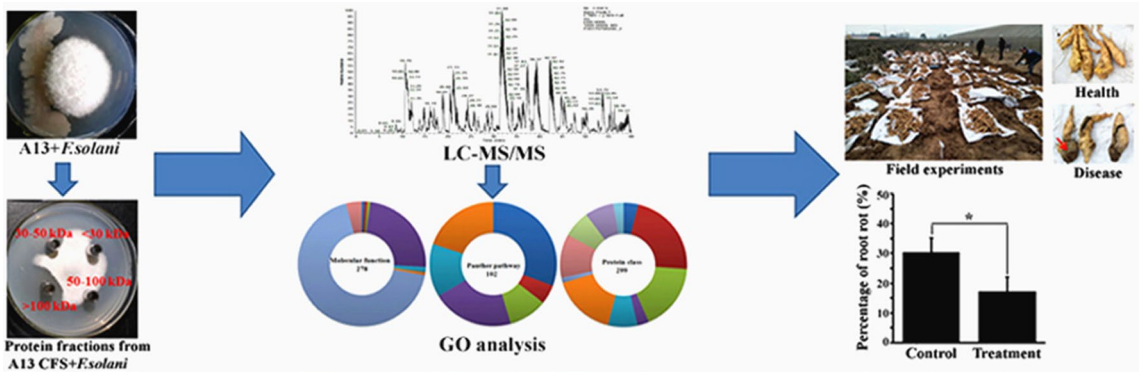

Background

As a promising alternative to crop protection chemicals, biocontrol of plant pathogens has ignited worldwide interest for its safety towards human health and its environment-friendly nature [1]. Different microbial genera (such as the bacteria *Bacillus* and *Pseudomonas*, and the fungus *Trichoderma*) have been reported as potential biocontrol agents against phytopathogens [2]. Among these, members of the genus *Bacillus*, consisting of 380 species [3], have proved to be an important source of biocontrol agents due to their distinctive abilities to form extreme environment-resistant endospore and produce a range of antimicrobial compounds [4].

At present, only a small proportion, of about 20 *Bacillus* species, mainly *B. subtilis*, *B. thuringiensis*, *B. amyloliquefaciens*, *B. pumilus* and *B. cereus*, have been investigated for biocontrol activity against phytopathogens [4, 5]. Moreover, owing to their genetic and metabolic diversity, different *Bacillus* species, even different strains belonging to the same species, can have markedly different inhibitory efficiencies and/or mechanisms against phytopathogens. For example, *Bacillus subtilis* M4 induced defense response in soybean against *Macrophomina phaseolina*, mediated by activities of antioxidant defense enzymes, such as superoxide dismutase, phenol peroxidase, peroxidase, and catalase [6], whereas *Bacillus subtilis* KLBC BS6 could also induce resistance defense response in blueberry against *Botrytis cinerea*, but mediated by other enzymes, such as chitinase, phenylalanine ammonia-lyase, and polyphenol oxidase [7]. *B. pumilus* W-7 from potato antagonized *Phytophthora infestans* by secreting surfactin and fengycin B [8], whereas *B. pumilus* MSUA3 from *Fagopyrum esculentum* strongly antagonized *Rhizoctonia solani and F. oxysporum* by producing chitinolytic enzymes and surfactin [9]. *Bacillus amyloliquefaciens* L3 from the watermelon produced two volatile organic compounds which inhibited *F. oxysporum* f.sp. *niveum* [10], whereas *B. amyloliquefaciens* 35 from cacao produced 10 different volatile organic compounds inhibiting mycelium growth and spore germination of *Moniliophtora roreri* [11]. All these researches suggests that it is important to investigate the biocontrol potential of some new *Bacillus* isolates, especially from under-evaluated *Bacillus* spp. Notably, these *Bacillus* strains in researches above were often isolated from different plants, suggesting that an effective strategy to broaden the scope of biocontrol agents is to isolate new bacterial strains within the genus *Bacillus* from different host plants.

Medicinal plants have been attracting increasing attentions due to their various pharmacological properties. In proper culture conditions, each medicinal plant would produce unique and structurally divergent bioactive secondary metabolites [12], some of which are frequently released into soil, shaping distinct and highly specific rhizosphere microbiome by attracting and maintaining a preferential soil microbial reservoir [13, 14]. In turn, rhizosphere microbiome can achieve direct or indirect protection for the host medicinal plant by improving the nutrient absorption, enhancing disease resistance, etc. [15, 16]. Despite the above advances, the bacteria from medicinal plant rhizosphere have not been widely explored for the use as new biocontrol agents.

R. glutinosa is one of the most important traditional Chinese medicinal herbs. It prefers to grow in the environment with sufficient light, sandy loam and good drainage, and release various root exudates (e.g., phenolic acid, phenylethanoid glycosides, and iridoid glycoside) into soil [17], which probably induce the colonization of some special functional microbes in *R. glutinousa* rhizosphere. In addition, during standard cultivation of *R. glutinosa*, root-rot disease frequently leads to yield losses of 10–80% each year. Therefore, isolating antagonistic microbes (e.g., new *Bacillus* strain) from the rhizosphere of healthy *R. glutinousa* will greatly facilitate the development of new

biological control agents active against root-rot disease of *R. glutinousa* or other medicinal plants.

To achieve the goal, in this study, 106 bacteria strains were isolated from the *R. glutinosa* rhizosphere. Among these strains, one new *B. tequilensis* strain A13 displayed the strongest biocontrol potential against root-rot pathogen, *F. solani*. Furthermore, protein fractionation, LC–MS/MS and GO bioinformatics analyses were performed to identify the extracellular protein components from A13 and the potential pathways by which these proteins inhibited the growth of *F. solani*.

Materials and methods

Isolation of bacteria from the rhizosphere soils of *R. glutinosa*

To isolate the bacteria, 10 g of *R. glutinosa* rhizosphere soil was placed in 100-mL sterile water and shaken at 180 rpm and 37 °C. After 30 min, the 100 µL suspension was spread on Luria–Bertani (LB) agar plate. After 48 h at 37 °C, bacterial colonies of different sizes, colors and morphologies appeared on the plates, were purified by streaking and stored at − 80 °C in LB broth supplemented with 50% glycerol.

Screening for the antagonistic bacteria against *F. solani*

All the isolates were screened for antagonism against the pathogenic fungus *F. solani* from *R. glutinosa*. Briefly, *F. solani* was cultured on potato dextrose agar (PDA) medium at 28 °C. After 4 days, a mycelial plug (5.0 mm in diameter) of *F. solani* was cut from the leading edge of the colony and transferred onto a new PDA plate. Then, one isolate was streaked in a straight line along one edge of the PDA plate; another plate was inoculated with only *F. solani* to use as a control. After 4 days at 28 °C, the inhibitory activity of each isolate was calculated as described by Kumar et al. [18]. Ultimately, strain A13, identified as having the greatest inhibitory ability, was selected for further study.

Strain characteristics and identification

The physiological characteristics of strain A13, including spore formation, gram staining, and gelatin liquefaction, were determined in accordance with Bergey's Manual of Determinative Bacteriology. The strain A13 was further identified by 16S rDNA sequencing using primers 27F (5′-AGAGTTTGATCCTGGCTCAG-3′)/1492R (5′-GGTTCCTTGTTACGACTT-3′). The total PCR reaction volume was 25 µL, containing 2 µL template DNA of the isolate bacteria, 12.5 µL of 2 × Taq PCR MasterMix, 0.8 µL of 10 µmol/L upstream and downstream primers and distilled water to a constant volume.

In accordance with the melting temperature values of the primers, the PCR amplification was started with predenaturation at 95 °C for 5 min, followed 35 cycles of denaturing at 94 °C for 30 s, annealing at 55 °C for 1 min and extension at 72 °C for 60 s, followed by holding the reaction mixture at 72 °C for 60 s to allow the complete extension of PCR products. PCR amplification products were stored at 4 °C and detected by electrophoresis on 1% agarose gels. They were then sequenced by the Sangon Biotech Company Limited (Shanghai, China).

Antifungal activity analysis of strain A13's cell-free supernatant (CFS)

The isolated bacteria A13 was grown in liquid LB medium with continuous shaking at 180 rpm and 28 °C for 48 h. The CFS was collected at 12-h intervals by centrifugation at 10,000 rpm for 10 min at 4 °C and then passed through a 0.22-µm pore size Millipore filter to remove any cellular debris. To determine the effects of different CFS contents on antifungal activity, 0.1, 0.5, 1, 2, 3, 4, 5, 6, 7, 8, 9, or 10 mL CFS was independently mixed with PDA medium to obtain 100 mL constant volume and spread independently on 90-mm plates. Mycelial disks (5 mm in diameter) from 5-day-old fungal cultures were placed in the center of each plate. After 3–5 days at 28 °C, the diameters of the colonies were measured, and the antifungal activity of the CFS at different times was calculated. The PDA plate without CFS, but inoculated with a mycelial disk was used as the control. The experiments were repeated three times.

Effects of temperature, pH and proteases on the antifungal activity of A13 CFS

To confirm its thermal stability, the CFS was maintained independently at 30, 40, 50, 60, 70, 80, 90, 100, and 120 °C for 120 min and then cooled to room temperature. To determine pH resistance, the pH of the CFS was adjusted from 3 to 11 using 1 M HCl or 1 M NaOH [19]. To evaluate protease resistance, the CFS was treated with 1, 5 and 10 mg/mL protease (protease K/trypsin) at 37 °C for 120 min. After these treatments, the effects of temperature, pH and proteases on the antifungal activity of the CFS were determined. The experiments were repeated three times.

Fractional extraction of the CFS proteins by ammonium sulfate precipitation and the fractions' antifungal activities

Proteins of the CFS were fractioned with ammonium sulfate at saturations of 10%, 20%, 30%, 40%, 50%, 60%, 70%, 80%, 90%, and 100% as described by Zhang et al. [20]. The different protein fractions were separately re-dissolved in phosphate buffer solution (pH 7.0) and desalinated by dialysis. Afterwards, 5-mm mycelial plugs from the 5 days old fungal colony were cut and transferred to PDA plates. Then, sterile Oxford Cups

(6 mm in internal diameter and 10 mm high) were placed around the mycelial plugs. The different protein fractions were added independently into different cups. The fraction with the strongest antifungal activity was selected to perform LC–MS/MS analysis.

LC–MS/MS analysis of antifungal proteins

The fraction with the strongest antifungal activity was further fractioned in an ultrafiltration tube using 30-, 50-, and 100-kDa molecular weight cutoff membranes. The inhibitory activities of the protein fractions with molecular weights of < 30 kDa, 30–50 kDa, 50–100 kDa, and > 100 kDa were analyzed using the diffusion experiment with the Oxford Cup method. The compositions of the fractions exhibiting antifungal activity were stored on dry ice and sent to Shanghai Zhong Ke New Life Company for LC–MS/MS (LC: Easy-nLC 1000, Thermo Fisher, USA; MS/MS: Q Exactive, Thermo Fisher, USA) detection. Specifically, 30 μg protein was added into 30 μl STD buffer (4% sodium dodecyl sulfate, 100 mM dithiothreitol, 150 mM Tris–HCl and pH 8.0). After 5 min incubation in a boiling water bath, the dilution was mixed with 200 μL UA buffer (8 M urea, 150 mM Tris–HCl and pH 8.0) in an 30 kDa ultrafiltration tube for centrifugation (14,000×*g*). The protein pellet was resuspended in 100 μL 50 mM iodoacetamide and incubated in darkness. After 30 min, the protein was successively washed with 100 ml UA buffer and 25 mM NH_4HCO_3. Then, the protein was resuspended in 40 μL 25 mM NH_4HCO_3 containing 2 μg trypsin for 24 h at 37 °C, followed by centrifugation. Finally, 40 μL of 25 mM of NH_4HCO_3 was added, and the mixture was through centrifugation and acidification.

Protein samples were separated by Easy-nLC system at a flow rate of 300 nL/min. Mobile phases A and B were 0.1% formic acid in high-performance liquid chromatography grade water and 0.1% formic acid in 84% acetonitrile, respectively. The linear gradient was 0–60% buffer B for 50 min, 60–90% buffer B for 4 min, held in 90% buffer B for 6 min. The eluted proteins were detected by MS and MS/MS. Under positive ion mode, the 20 most abundant precursor ions were selected from the survey scan (300–1800 m/z) for high-energy collisional dissociation fragmentation. Survey scans were acquired at a resolution of 70,000 at m/z 100 and the resolution for high-energy collisional dissociation spectra was set to 17,500 at m/z 100. Normalized collision energy was 27 eV and the underfill ratio was defined as 0.1%. A raw data file was submitted to UniProtKB database [21] to obtain the qualitative identification information of the target polypeptide molecules.

Field experiments

In field experiments, two treatments (five parallel fields/each treatment) were arranged a week before *R. glutinosa* planting: (1) Treatment group: complex fertilizer (5 kg, Nuoweier Fertilizer Company Limited, China) combined with A13 (3.2×10^{13} cells) was spread on the field (22 m^2); (2) Control group: 5 kg complex fertilizer alone was spread on the field (22 m^2). The total nitrogen, phosphorus and potassium contents in the complex fertilizer were each > 45%. At harvesting stage, a total of > 110 roots for control or treatment field were randomly selected to count the root-rot incidence of *R. glutinosa*.

Statistical analysis

All statistical analyses were performed using origin 6.0 or excel 2010 software. Student's *T* test was used for statistical comparison and $P < 0.05$ was considered to be a significant difference. A GO enrichment analysis of antifungal proteins was performed using the Gene Ontology database [22].

Results

Inhibitory effects of isolate A13 on *F. solani* growth

We obtained 106 isolates of bacteria from the rhizosphere soil of *R. glutinosa*. Among these isolates, isolate A13 displayed the strongest *in vitro* inhibitory activity against *F. solani* growth, achieving 73.49% ± 1.33% inhibition (Fig. 1A, B). After being inoculated into sterilized soil, the CFU (colony forming units) number for A13 in the soil increased from $(3.43 \pm 0.59) \times 10^8$ CFU/g at day 0 to $(1.04 \pm 0.20) \times 10^9$ CFU/g at day 90, suggesting that A13 survived in the soil environment, which is important for a microbial agent that is to be used for the control of a soil-borne pathogen [23].

The isolate A13 characteristics and identification

After incubation on the agar culture medium for 48 h at 37 °C, the A13 colony exhibited milk white, wrinkled protuberances at the center and was opaque with an irregular edge. When observed using light microscopy, isolate A13 cells appeared rod-like (Additional file 1). The physiological characteristics of A13 were analyzed (Table 1). A13 produced positive results to most tests, such as spore formation, gram staining, and gelatin liquefaction, indicating that A13 belonged to the genus *Bacillus*. Furthermore, the 16S rDNA sequence indicated that isolate A13 showed 99.93% homology with strain *B. tequilensis* strain 10b (Accession number: NR_104919.1).

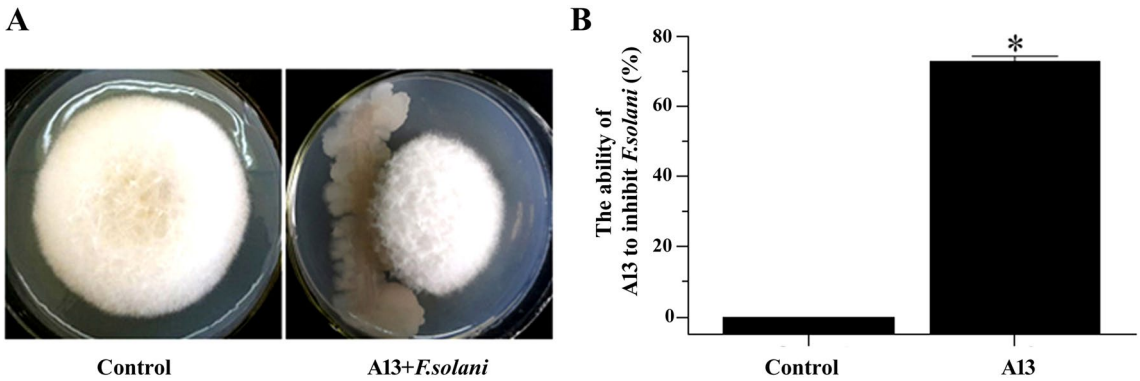

Fig.1 Antagonistic effect of isolate A13 on *F. solani*. **A**, **B** The growth inhibition of A13 to *F. solani*. *$P < 0.05$

Table 1 Physiological characteristics of strain A13

Characteristics	Reaction	Characteristics	Reaction
Spore formation	Positive	Starch hydrolysis	Positive
Gelatin liquefaction	Positive	Citrate test	Positive
Indole production	Positive	Methyl Red test	Negative
Nitrate reduction test	Positive	Voges Proskauer test	Positive
Lactose fermentation test	Negative	Urease test	Positive

Antifungal activity of B. tequilensis A13 CFS against F. solani

To examine the inhibitory effect of A13 CFS, *F. solani* was incubated on PDA plates containing 10% CFS for 3–5 days at 28 °C as described in "Materials and methods" section. As shown in Fig. 2A and B, CFS collected after 12 h, 24 h, 36 h, or 48 h of A13 growth (12 h-, 24 h-, 36 h-, or 48 h-A13 CFS) showed strong inhibitory effect on *F. solani* growth. Futhermore, 36 h-A13 CFS had the highest inhibitory ratio (up to 47.42%) against *F. solani*, although no significant difference was found between 36 h-A13 CFS and 24 h-/48 h- A13 CFS. As shown in Fig. 2C and D, the 36 h- A13 CFS inhibited the growth of *F. solani* in a concentration-dependent manner, with the average inhibitory activity increased from 12.29 to 47.42% along with the concentration range from 0.1% to 10%, respectively, suggesting that the extracellular substances from A13 contained antifungal compounds for which the concentration was positively correlated with inhibitory activity against *F. solani* growth.

Furthermore, we investigated the effects of different physicochemical conditions on the inhibitory activity of 36 h-A13 CFS on *F. solani* growth. As shown in Fig. 3A and B, after a 120 min heat treatment at different temperatures (30–100 °C), the average inhibitory activity of 36 h-A13 CFS on *F. solani* growth ranged from 41.74% to 52.91%. The inhibitory activity of 36 h-A13 CFS in initial pH values ranging from 5.0 to 11.0 changed from 28.78% to 45.85% (Fig. 3C, D). Thus, the inhibitory activity of 36 h-A13 CFS was maintained at a high level over wide pH (4.0–11.0) and temperature (30–100 °C) ranges, although the antifungal activity varied with changes in pH or temperature. This stability at different pH levels and temperatures is helpful for the preservation and application of 36 h-A13 CFS when compared with traditional biological pesticides [24]. On the other hand, the inhibitory activity of 36 h-A13 CFS was severely negatively affected by proteolytic enzymes, such as proteinase K and trypsin. As shown in Fig. 3E and F, the addition of proteases decreased the inhibitory activity of 36 h-A13 CFS in a concentration-dependent manner. Both trypsin and proteinase K-treated CFS displayed significant lower inhibitory ability at a 10 mg/mL concentration than that at 1 and 5 mg/mL concentrations. Further, at a 10 mg/mL concentration, trypsin and proteinase K reduced the average inhibitory activity of 36 h-A13 CFS to 19.07% and 28.35%, respectively. Extracellular proteins play several very important roles in promoting plant growth and killing plant pathogens [25]. Thus, we speculated that some protein molecules were important for the inhibitory activity of 36 h-A13 CFS.

Bioinformatics analysis of A13 CFS protein fractions having inhibitory activities against *F. solani*

Protein fractions of 36 h-A13 CFS were obtained by salting-out with ammonium sulfate at saturations of 10%–100%. As shown in Additional file 2A, the inhibitory activities of proteins against *F. solani* varied with different ammonium sulfate saturation levels, and the protein precipitation obtained by 70% saturated ammonium sulfate displayed the strongest inhibitory activity (Additional file 2A). This was further fractioned into four subfractions using microporous membranes:

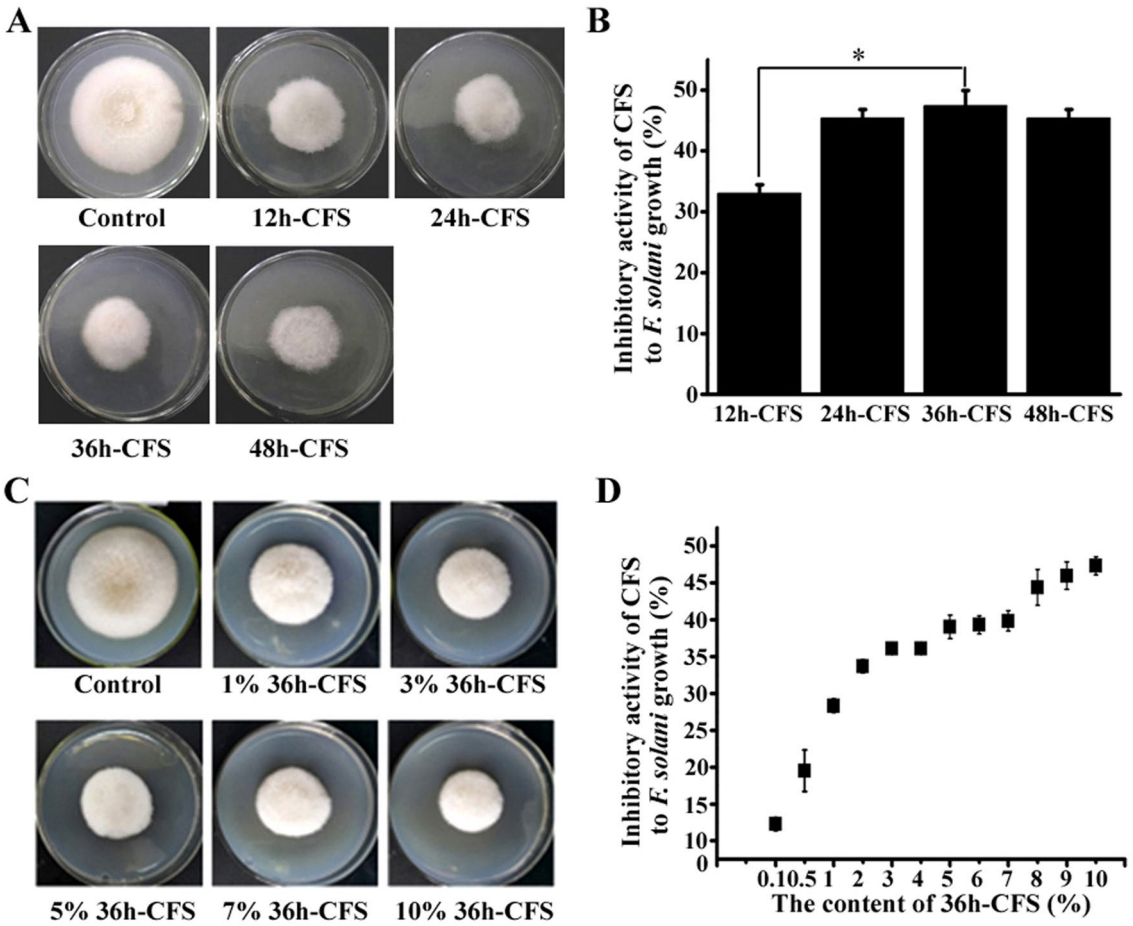

Fig. 2 Antifungal activity against *F. solani* of A13 CFS. **A**, **B** antifungal activity of CFS collected at different times of A13 growth; **C**, **D** antifungal activity of different ratios of CFS collected after 36 h of A13 growth. *$P < 0.05$

fraction A (< 30 kDa), fraction B (30–50 kDa), fraction C (50–100 kDa) and fraction D (> 100 kDa). Of these, only fractions B and D obviously inhibited *F. solani* growth (Additional file 2B).

To screen the potential protein components capable of inhibiting *F. solani* growth, we performed LC–MS/MS and bioinformatics analysis using GO bioinformatics resources. LC–MS/MS profiles of fractions B (30 − 50 kDa) and D (> 100 kDa) from *B. tequilensis* A13 are shown in Additional file 3. Furthermore, a total of 1,353 extracellular proteins of *B. tequilensis* A13 were identified in fractions B and D. Among these proteins, 500 proteins were annotated with 278, 299 and 102 terms corresponding to 8, 16 and 49 categories of molecular function, protein class and PANTHER pathway, respectively. In detail, the top categories for molecular function were catalytic activity (68%), binding (23.7%) and transporter activity (4.0%). Consistent with the molecular function, the top categories for protein class were enzymes (78%) and nucleic acid-binding proteins (11.4%). Among the enzymes, hydrolases possessed 22.4% of the total protein classes and were the most common proteins (Fig. 4). Further analysis indicated that six antimicrobial proteins, namely subtilisin, beta-1,3–1,4 glucanase, lysozyme, iturin, antimicrobial peptide LCI, and putative antimicrobiological protein were present among the A13 extracellular proteins. Notably, among the identified ligases, some synthetases of cyclic lipopeptide antibiotics and bacitracin with strong inhibition activities against pathogenic fungi, such as plipastatin, surfactin, mycosubtilin, fengycin, and linear gramicidin, were also detected in this study, suggesting that A13 has the ability to produce these antimicrobial compounds. The proteins in A13 CFS associated with plant pathogen inhibition are listed in Table 2.

A metabolic pathway analysis indicated that amino acid-, vitamin-, and plant stress resistance-related metabolic categories possessed 30.60%, 5%, and 9.80% of the total 49

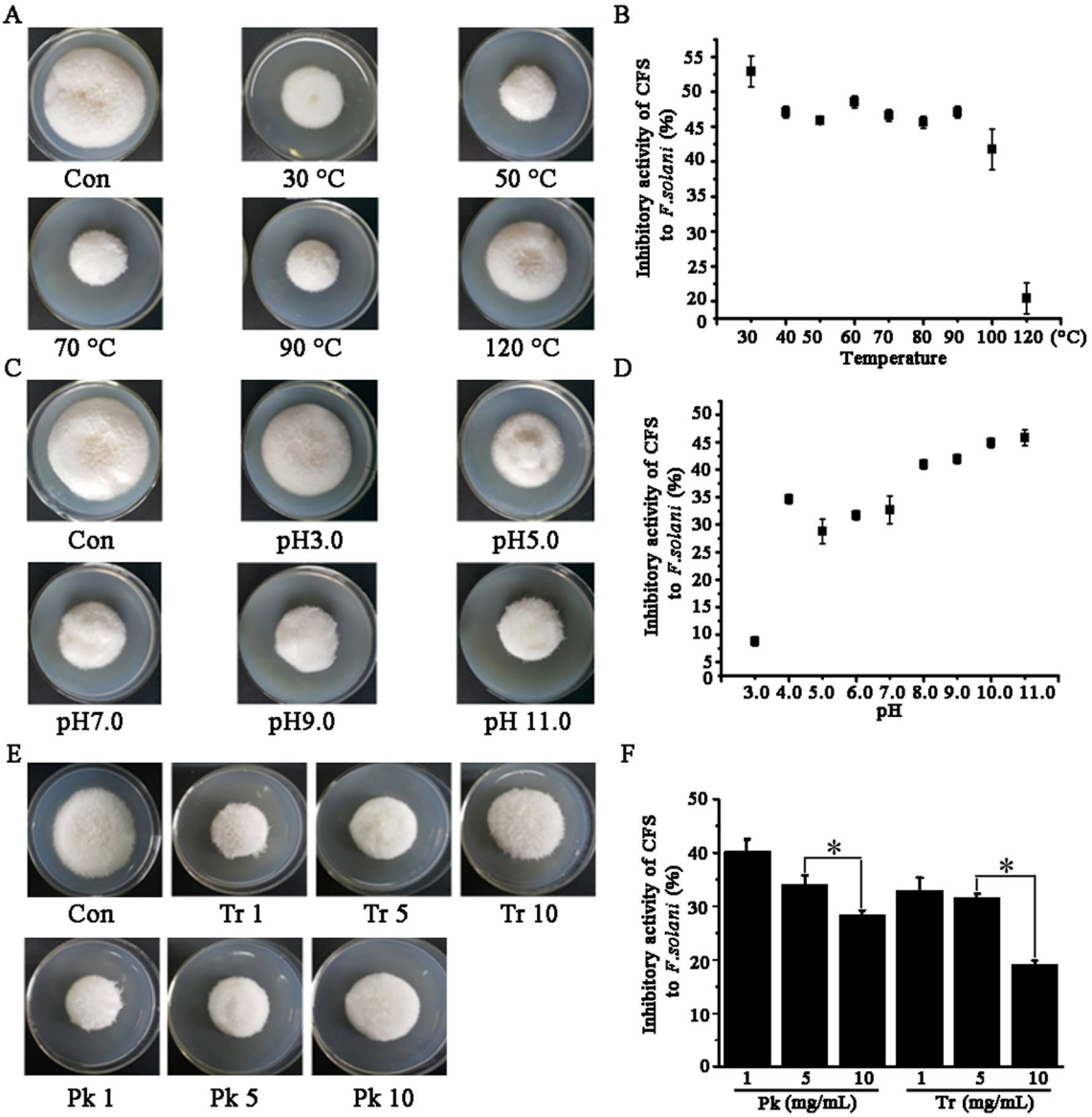

Fig. 3 The effect of physicochemical properties and proteinases on inhibitory activity of A13 CFS against *F. solani*. **A**, **B** the effect of temperature; **C**, **D** the effect of pH; **E**, **F** the effect of different proteinases. Con, control; Tr 1–10 and Pk1-10 represent trypsin 1–10 mg/mL and proteinase K 1–10 mg/mL, respectively. *$P < 0.05$

metabolic categories, respectively (Fig. 4). Furthermore, extracellular proteins of A13 were involved in the biosynthesis of 15 amino acids, namely phenylalanine, arginine, valine, methionine, tyrosine, lysine, threonine, isoleucine, histidine, serine, glycine, s-adenosylmethionine, cysteine, proline, and tryptophan, as well as five vitamins, thiamin, vitamin B6, flavin, biotin, and tetrahydrofolate. In addition, it has been found that some extracellular proteins of A13 were involved in plant stress resistance-related metabolisms, such as aminobutyrate and 5-hydroxytryptamine metabolic pathways.

A field application of *B. tequilensis* A13 for the biocontrol of *R. glutinosa* root-rot disease

The inoculation experiment revealed that the root-rot disease incidence in the tests simultaneously inoculated with both *F. solani* and *B. tequilensis* A13 was reduced by 42.85% when compared with the value from the test inoculated with only *F. solani*. Furthermore, when A13 at a density of 6.4×10^9 CFU/g was combined together with complex fertilizer and applied in the fields, the average root-rot disease incidence of *R. glutinosa* decreased by 13.13%, when compared with the control group (Fig. 5).

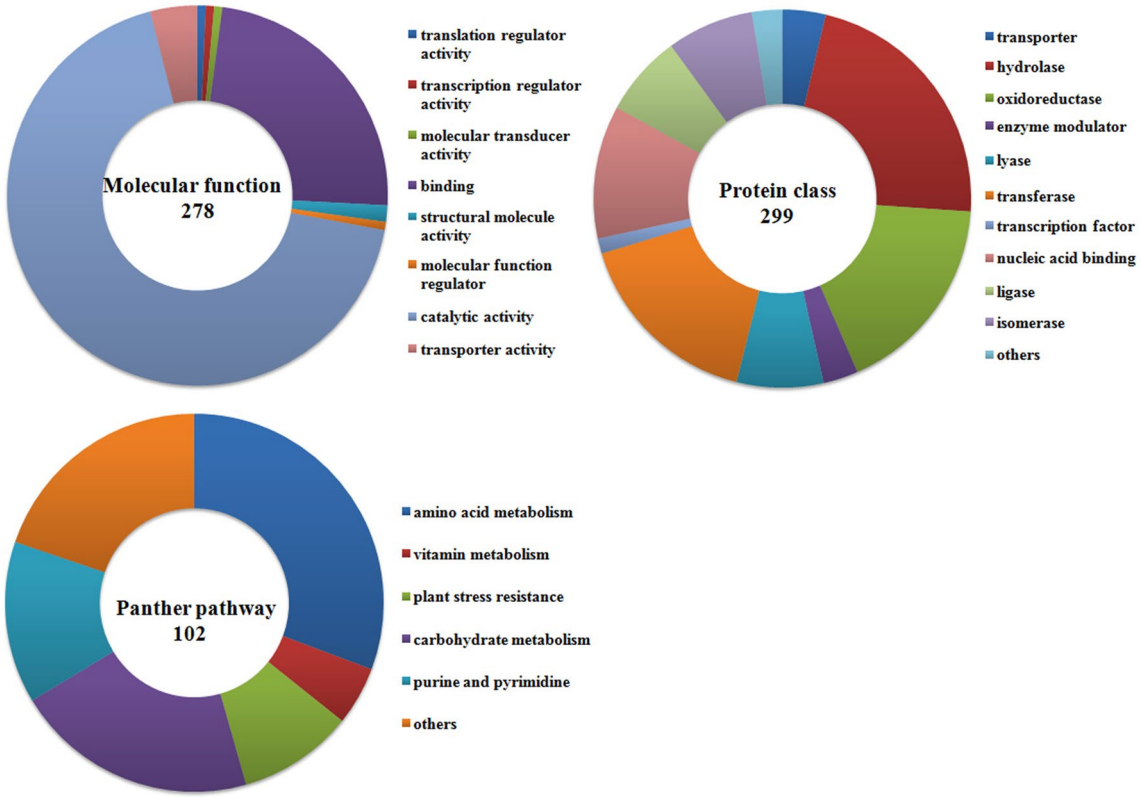

Fig. 4 GO analysis of antifungal protein fractions from A13 CFS

Table 2 The proteins related with plant pathogen inhibition in *B. tequilensis* A13 CFS

Protein name	Pep Count	Unique Pep Count	Protein ID
Subtilisin (Peptidase S8)	65	38	tr|A0A1A0FUH6/tr|A0A1D8FNB7/ tr|A0A1D8FK42/ tr|A0A1D8FIT1
Putative antimicrobiological protein	43	13	tr|A0A0A0RBJ1
Beta-1,3–1,4 glucanase	10	8	tr|D4G3N4
Fengycin synthetase	5	4	tr|D0EX65/ tr|O30980/ tr|H9TE67
Mycosubtilin synthase	3	3	tr|A0A1A0CYP2/ tr|A0A1A0CB76
Surfactin synthetase	3	3	tr|A0A0D1L592/ tr|G4F048/ tr|A0A068PS98
Subtilosin biosynthesis protein	2	2	tr|I2C5B3
Lysozyme (Lysostaphin)	2	2	tr|M5P7M9/ tr|L8AHK2
Iturin A	1	1	tr|X5FP79
Antimicrobial peptide LCI	1	1	tr|A0A1A0CXQ4
Plipastatin synthase subunit E	1	1	tr|G9LQ51
Linear gramicidin synthetase	1	1	tr|I2C5F0
Lanthionine synthetase	1	1	tr|R9R8B8
Fusaricidin synthetase	1	1	tr|M5PAP1

Discussion

As a promising alternative to chemical fungicides, the biocontrol of plant pathogens has been attracting attention. However, obtaining a strain with high biocontrol ability against a pathogenic fungus is becoming a key constraint for the biological control of plant diseases. Currently, an effective strategy to broaden the scope of biocontrol agents is to isolate novel bacterial strains from different plants in which traditional Chinese medicinal

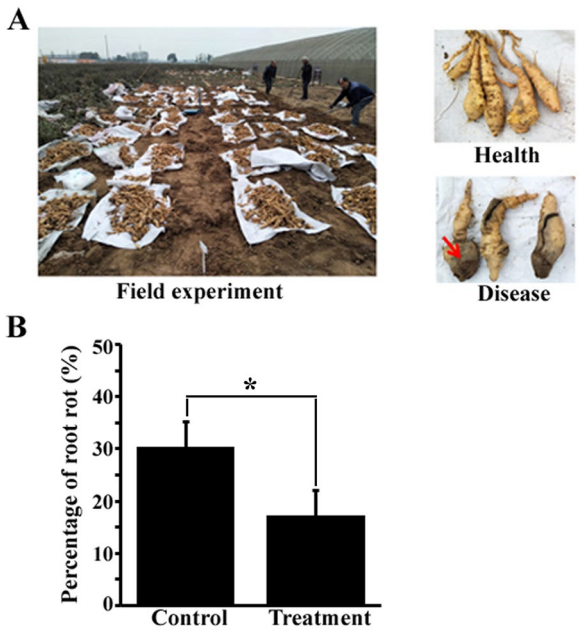

Fig. 5 The effect of complex fertilizer combined with A13 on *R. glutinosa* root rot in the fields. **A** The field experiment of complex fertilizer (Control); **B** the influence of complex fertilizer combined with A13 (Treatment) on incidence of *R. glutinosa* root rot. *$P < 0.05$

herbs, such as *R. glutinosa,* should be targeted due to their growth characteristics and unique root exudates.

In this study, 18 of 106 bacteria isolated from *R. glutinosa* rhizosphere displayed obvious antagonistic activities against the root-rot pathogen *F. solani* (average inhibitory ratio: 65.78%–73.49%). Among these 18 bacteria, *B. tequilensis* A13 displayed the strongest inhibitory activity (73.49% ± 1.33%) against *F. solani* in confrontation experiments, maintained an effective survival rate in sterilized soil and reduced the incidence of *R. glutinosa* root rot by 42.85% in the inoculation experiments. When *B. tequilensis* A13 was used together with a complex fertilizer in field experiments, the average incidence of root rot was significantly reduced in *R. glutinosa* (Fig. 5). Of course, further field experiments should be conducted to determine the optimum frequency, dose and timing of *B. tequilensis* A13 application. This is the first report of isolation of *B. tequilensis* A13 from Chinese medicinal plant *R. glutinosa* and demonstration of its antagonistic activities against the root-rot pathogen *F. solani*.

B. tequilensis is widely found in soil and water and degrades various organic contaminations [26–28] by producing extracellular enzymes. Recently, different strains of *B. tequilensis* were isolated from different plant and confirmed to possess the ability to promote plant growth or inhibit the growth of microorganisms. For example, Bhattacharya et al. indicated that endophytic *B. tequilensis* PBE1 isolated from tomato can effectively inhibit mycelial growth of *F. oxysporum* inducing tomato wilt disease and promoted tomato growth by producing indole acetic acid and hydroxymate type siderophore [29]; Nagrale et al. reported that *B. tequilensis* CICR-H3 isolated from cotton displayed 62.84 ± 0.50% inhibition ratio against *Macrophomina phaseolina* inducing cotton root rot by producing volatile organic compounds, such as Benzene, 1, 3-diethyl- and Benzene, 1, 4-diethyl [30]; Kumar et al. isolated the *B. tequilensis* KAS3 from *Pennisetum glaucum* L. which significantly protected seedlings from *Fusarium* sp. infection by producing lipopeptide [31]. Although the recent significant advances, only few studies are available on activity and mechanism of *B. tequilensis* acting as a biological control agent against phytopathogenic fungi inducing root-rot disease of medicinal plants.

Saoussen pointed out that producing antipathogenic metabolites was the best known and most important mechanism that allowed antagonistic microorganisms to inhibit plant pathogens [32]. Thus, in this study, we performed the LC–MS/MS and bioinformatics analyses of extracellular proteins from *B. tequilensis* A13. The results indicated that *B. tequilensis* A13 was capable of producing six compounds capable of antagonizing phytopathogenic fungi: subtilisin, beta-1,3–1,4 glucanase, lysozyme, iturin, antimicrobial peptide LCI, and putative antimicrobiological protein. For example, a subtilisin-like serine proteinase rTghSS42 exhibited broad-spectrum antifungal activity against *F. oxysporum*, *Alternaria alternate*, etc. by inhibiting mycelial growth [33]. Beta-1,3–1,4 glucanase caused deformity, bending, and breakage of the mycelia in both *Botrytis cinerea* and *Alternaria panax* by the hydrolyzing β-1, 3–1, 4-glucan in cell wall [34]. Antimicrobial peptide LCI inhibited the growth of both *F. moniliforme* and *F. solani*, which might be achieved by interacting with cell membranes; thus, increasing membrane permeability [35, 36]. Furthermore, we also found that A13 produced various synthetases of antimicrobial compounds, such as plipastatin, surfactin, mycosubtilin, fusaricidins, and fengycin, which were highly efficient against phytopathogenic fungi from genus *Fusarium* and other genera. For example, surfactin from *Brevibacillus brevis* inhibited the hyphal growth of the phytopathogenic fungi *F. moniliforme* by damaging its DNA and proteins and reducing its glutathione content [37]. Surfactin C from *B. velezensis* strain 1B-23 and *Bacillus* sp. strain 1D-12 significantly reduced the disease incidence of bacterial canker caused by *Clavibacter michiganensis* subsp. *Michiganensis* in tomato [38]. Fusaricidins, potent antifungal biocontrol agents against a broad array

of phytopathogenic fungi, have frequently been used to treat plant diseases, such as fusarium wilt of cucumber and gibberella ear rot of maize [39]. Therefore, various antimicrobial compounds that were produced by *B. tequilensis* A13 may have cooperatively inhibited the growth of *F. solani*. Moreover, these compounds may also antagonize other pathogens, which was supported by *B. tequilensis* A13 obviously inhibiting the growth of phytopathogenic fungi *Penicillium janthinellum* and *Aspergillus tubingensis* (Additional file 4). In addition, our results indicated that some extracellular proteins of *B. tequilensis* A13 were involved in the synthetic pathways of 15 amino acids and five vitamins, as well as two plant stress-response pathways. Thus, it is possible that *B. tequilensis* A13 has multiple mechanisms by which to inhibit phytopathogenic fungi inducing root-rot and to maintain plant health.

Based on all the data, the novel strain *B. tequilensis* A13 showed highly effective and broad biocontrol activities against phytopathogenic fungi, especially *F. solani*. LC–MS/MS and GO analysis of extracellular proteins indicated that the strain could produce several antifungal compounds, which may target different species of pathogens or different pathogenesis mechanisms to play antifungal roles. This study enhanced the understanding of the antifungal mechanism in genus *Bacillus* and provided an excellent candidate biocontrol agent. In addition, the *B. tequilensis* A13 was first isolated from *R. glutinosa* rhizosphere, which highlighted medicinal plants as new resource pools for microorganisms with potential for developing into biocontrol agents.

Conclusion

In conclusion, among members of the genus *Bacillus*, the biocontrol efficiency of *B. tequilensis* against plant fungal diseases, such as root rot, has been rarely explored. In this study, we isolated a novel strain, *B. tequilensis* A13, from *R. glutinosa* rhizosphere and investigated its biocontrol potential against *R. glutinosa* root-rot pathogen *F. solani*. Our study found the following: (1) *B. tequilensis* A13 significantly inhibited the growth of *F. solani* inducing *R. glutinosa* root-rot disease; (2) *B. tequilensis* A13 significantly reduced the incidence of *R. glutinosa* root-rot disease in inoculation and field experiments; and (3) *B. tequilensis* A13 produced several antifungal compounds, such as beta-1,3–1,4 glucanase, subtilisin, and antimicrobial peptide LCI, which contribute to the antifungal activity of *B. tequilensis* A13. Therefore, *B. tequilensis* A13 is a promising candidate for development into a biocontrol agent against *R. glutinosa* root-rot disease.

Abbreviations

LC–MS/MS	Liquid chromatography electrospray ionization tandem mass spectrometry
GO	Gene Ontology
LB	Luria–Bertani
PDA	Potato dextrose agar
CFU	Colony forming units
CFS	Cell-free supernatant
Rehmannia glutinosa	*R. glutinosa*
Fusarium solani	*F. solani*
Bacillus tequilensis	*B. tequilensis*

Supplementary Information

The online version contains supplementary material available at https://doi.org/10.1186/s40538-023-00390-y.

Additional file 1. Colony and microscopic morphology of the strain A13.**Additional file 2.** The inhibitory activity of protein fractions from A13 CFS. **A** the inhibitory activity of protein fractions obtained from CFS by different ammonium sulfate concentrations; **B** the inhibitory activity of protein fraction obtained from CFS by 70% ammonium sulfate concentration. The protein fraction was further divided into four fractions: fraction A (< 30 kDa), fraction B (30–50 kDa), fraction C (50–100 kDa) and fraction D (> 100 kDa).**Additional file 3.** LC–MS/MS profiles of protein components of fraction B (30–50 KD) and fraction D (> 100 KD). **A** fraction B; **B** fraction D.**Additional file 4. B. tequilensis** A13 inhibited the growth of *Penicillium janthinellum* and *Aspergillus tubingensis*.

Acknowledgements

We thank International Science Editing (http://www.internationalscienceediting.com) for editing this manuscript.

Author contributions

RW performed project administration and writing-original draft, arranged funding sources. HL performed the lab experiments. ZQ performed the field experiments. YW performed data duration. QY supervised the study and writing of the manuscript, arranged funding sources. HZ arranged funding sources, contributed in review and editing of the manuscript. ML contributed in review and editing of the manuscript. All authors read and approved the final manuscript.

Funding

This work was supported by China Agriculture Research System (CARS-21); The Zhongyuan high level talents special support plan-Science and Technology Innovation Leading Talents (224200510011); The Key Science and Technology Project of Henan Province, China (202102110219); Educational Commission of Henan Province of China (22B180006, 20A180015).

Availability of data and materials

The data used and/or analyzed during the current study are available from the corresponding author on rational request.

Declarations

Ethics approval and consent to participate

Not applicable.

Consent for publication

All the authors gave their consent for publication of this article.

Competing interests

The authors declare that there is no competing interest among the authors.

Author details

[1]College of Life Sciences, Henan Normal University, Jianshe Road 46, Xinxiang 453007, China. [2]Henan International Joint Laboratory of Agricultural

Microbial Ecology and Technology, Xinxiang 453007, China. [3]Engineering Technology Research Center of Nursing and Utilization of Genuine Chinese Crude Drugs in Henan Province, Xinxiang 453007, China.

Received: 31 October 2022 Accepted: 7 February 2023
Published online: 02 March 2023

References

1. Nguyen DT, Nguyen CH, Nguyen HV, Hoang TBT, Chetan K, Pham VT, Trinh XH. Biological control of fusarium root rot of Indian mulberry (*Morinda ofcinalis* How.) with consortia of agriculturally important microorganisms in Viet Nam. Chem Biol Technol Agric. 2019;6:27. https://doi.org/10.1186/s40538-019-0168-x.
2. Corato UD. Soil microbiota manipulation and its role in suppressing soil-borne plant pathogens in organic farming systems under the light of microbiome-assisted strategies. Chem Biol Technol Agric. 2020;7:17. https://doi.org/10.1186/s40538-020-00183-7.
3. Fernandes FMR, Ribeiro TG, Rouws JR, de Barros Soares LH, Zilli JÉ. Biotechnological potential of bacteria from genera *Bacillus Paraburkholderia and Pseudomonas* to control seed fungal pathogens. Brazil J Microbiol. 2021;52:705–14. https://doi.org/10.1007/s42770-021-00448-9.
4. Dame ZT, Rahman M, Islam T. *Bacilli* as sources of agrobiotechnology: recent advances and future directions. Green Chem Lett Rev. 2021;14:246–71. https://doi.org/10.1080/17518253.2021.1905080.
5. Shafi J, Tian H, Ji MS. Bacillus species as versatile weapons for plant pathogens: a review. Biotech Biotech Equip. 2017;31:446–59. https://doi.org/10.1080/13102818.2017.1286950.
6. Chauhan P, Bhattacharya A, Giri VP, Singh SP, Gupta SC, Verma P, Dwivedi A, Rajput LS, Mishra A. *Bacillus subtilis* suppresses the charcoal rot disease by inducing defence responses and physiological attributes in soybean. Arch Microbiol. 2022;204:266. https://doi.org/10.1007/s00203-022-02876-z.
7. Lu YY, Ma DT, He X, Wang F, Wu JR, Liu Y, Jiao JY, Deng J. *Bacillus subtilis* KLBC BS6 induces resistance and defence-related response against *Botrytis cinerea* in blueberry fruit. Physiol Mol Plant. 2021;114:101599. https://doi.org/10.1016/j.pmpp.2020.101599.
8. Wang YY, Zhang CY, Liang J, Wang L, Gao WB, Jiang JZ, Chang RX. Surfactin and fengycin B extracted from Bacillus pumilus W-7 provide protection against potato late blight via distinct and synergistic mechanisms. Appl Microbiol Biotechnol. 2020;104:7467–81. https://doi.org/10.1007/s00253-020-10773-y.
9. Agarwal M, Dheeman S, Dubey RC, Kumar P, Maheshwari DK, Bajpai VK. Differential antagonistic responses of Bacillus pumilus MSUA3 against Rhizoctonia solani and Fusarium oxysporum causing fungal diseases in Fagopyrum esculentum Moench. Microbiol Res. 2017;205:40–7. https://doi.org/10.1016/j.micres.2017.08.012.
10. Wu YC, Zhou JY, Li YG, Ma Y. Antifungal and plant growth promotion activity of volatile organic compounds produced by Bacillus amyloliquefaciens. Microbiol Open. 2019;8:e00813. https://doi.org/10.1002/mbo3.813.
11. De la Cruz-López N, Cruz-López L, Holguín-Meléndez F, Guillén-Navarro GK, Huerta- PG. Volatile organic compounds produced by cacao endophytic bacteria and their inhibitory activity on *Moniliophthora roreri*. Curr Microbiol. 2022;79:35. https://doi.org/10.1007/s00284-021-02696-2.
12. Bhardwaj S, Sharma N, Negi S. Bioprospecting plant growth promoting rhizobacteria isolated from pharmacologically important medicinal plant *Acorus calamus* in Mid-Hill Himalayas. Mater Today Proc. 2022. https://doi.org/10.1016/j.matpr.2022.10.264.
13. Yuan YD, Zuo JJ, Zhang HanyueY, Zu MT, Liu S. The Chinese medicinal plants rhizosphere: metabolites, microorganisms, and interaction. Rhizosphere. 2022;22:100540. https://doi.org/10.1016/j.rhisph.2022.100540.
14. Sauer S, Dlugosch L, Kammerer DR, Stintzing FC, Simon M. The microbiome of the medicinal plants Achillea millefolium L and Hamamelis virginiana L. Front Microbiol. 2021;12:696398. https://doi.org/10.3389/fmicb.2021.696398.
15. Zhang YH, Zheng LL, Zheng Y, Xue S, Zhang JX, Huang P, Zhao YH, Hao XC, He ZK, Hu ZB, Zhou C, Chen QH, Liu JP, Wang GD, Sang M, Sun XD, Wang XB, Xiao X, Li C. Insight into the assembly of root-associated microbiome in the medicinal plant *Polygonum cuspidatum*. Ind Crop Prod. 2020;145:112163. https://doi.org/10.1016/j.indcrop.2020.112163.
16. Shokati B, Poudineh Z. An overview of plant growth promoting rhizobacteria and their influence on essential oils of medicinal plants: a review article. Iranian J Plant Physiol. 2017;7:2051–61. https://doi.org/10.22034/ijpp.2017.533559.
17. Zhang B, Weston LA, Li M, Zhu X, Weston PA, Feng F, Zhang B, Zhang L, Gu L, Zhang Z. *Rehmania glutinosa* replant issues: root exudate-rhizobiome interactions clearly influence replant success. Front Microbiol. 2020;11:1413. https://doi.org/10.3389/fmicb.2020.01413.
18. Kumar PN, Swapna TH, Khan MY. Statistical optimization of antifungal iturin A production from *Bacillus amyloliquefaciens* RHNK22 using agro-industrial wastes. Saudi J Biol Sci. 2017;24:1722–40. https://doi.org/10.1016/j.sjbs.2015.09.014.
19. Olorunjuwon O, Olubukola OB, Mobolaji A, Muibat OF, Temitope KB. Partial purification, characterization and application of bacteriocin from bacteria isolated *Parkia biglobosa* Seeds. Sciences. 2018;3(2):72–94. https://doi.org/10.28978/nesciences.424517.
20. Zhang XY, Li BQ, Wang Y, Guo QG, Lu XY, Li SZ, Ma P. Lipopeptides, a novel protein, and volatile compounds contribute to the antifungal activity of the biocontrol agent *Bacillus atrophaeus* CAB-1. Appl Microbiol Biotechnol. 2013;97:9525–34. https://doi.org/10.1007/s00253-013-5198-x.
21. UniProtKB database. www.uniprot.org. Accessed 10 May 2018.
22. Gene Ontology database. http://geneontology.org/. Accessed 20 July 2020.
23. Fathi F, Saberi-Riseh R, Khodaygan P. Survivability and controlled release of alginate-microencapsulated *Pseudomonas fluorescens* VUPF506 and their effects on biocontrol of *Rhizoctonia solani* on potato. Int J Biol Macromol. 2021;183:627–34. https://doi.org/10.1016/j.ijbiomac.2021.04.159.
24. Li H, Guan Y, Dong YL, Zhao L, Rong SH, Chen WQ, Lv MM, Xu H, Gao XL. Isolation and evaluation of endophytic *Bacillus tequilensis* GYLH001 with potential application for biological control of *Magnaporthe oryzae*. PLoS ONE. 2018;13:e0203505. https://doi.org/10.1371/journal.pone.0203505.
25. Chen L, Shi H, Heng JY, Wang DX, Bian K. Antimicrobial, plant growth-promoting and genomic properties of the peanut endophyte *Bacillus velezensis* LDO2. Microbiol Res. 2019;218:41–8. https://doi.org/10.1016/j.micres.2018.10.002.
26. Nadia ZJ, Hatem R, Mouna BE, Fatma ZR, Gorgi HC, Slimene BAH, Abdelmalek B, Abdessatar T, Samir B, Bassem J. A novel keratinase from *Bacillus tequilensis* strain Q7 with promising potential for the leather bating process. Int J Biol Macromol. 2015;79:952–64. https://doi.org/10.1016/j.ijbiomac.2015.05.038.
27. Angural S, Kumar A, Kumar D, Warmoota R, Sondhi S, Gupta N. Lignolytic and hemicellulolytic enzyme cocktail production from *Bacillus tequilensis* LXM 55 and its application in pulp biobleaching. Bioprocess Biosyst Eng. 2020;43:2219–29. https://doi.org/10.1007/s00449-020-02407-4.
28. Dar MA, Pawar KD, Chintalchere JM, Pandit RS. Statistical optimization of lignocellulosic waste containing culture medium for enhanced production of cellulase by *Bacillus tequilensis* G9. Waste Dispos Sustain Energy. 2019;1:213–26. https://doi.org/10.1007/s42768-019-00016-w.
29. Bhattacharya A, Giri VP, Singh SP, Pandey S, Chauhan P, Soni SK, Srivastava S, Singh PC, Mishra A. Intervention of bio-protective endophyte *Bacillus tequilensis* enhance physiological strength of tomato during Fusarium wilt infection. Biol Control. 2019;139:104074. https://doi.org/10.1016/j.biocontrol.2019.104074.
30. Nagrale DT, Gawande SP, Shah V, Verma P, Hiremani NS, Prabhulinga T, Gokte-Narkhedkar N, Waghmare VN. Biocontrol potential of volatile organic compounds (VOCs) produced by cotton endophytic rhizobacteria against Macrophomina phaseolina. Eur J Plant Pathol. 2022;163:467–82. https://doi.org/10.1007/s10658-022-02490-1.
31. Kumar K, Verma A, Pal G, White JF, Verma SK. Seed endophytic bacteria of pearl millet (*Pennisetum glaucum* L) promote seedling development and defend against a fungal phytopathogen. Front Microb. 2021;12:774293. https://doi.org/10.3389/fmicb.2021.774293.
32. Saoussen KB, Boutheina MT, Slim T. Biological potential of *Bacillus subtilis* V26 for the control of Fusarium wilt and tuber dry rot on potato caused by *Fusarium* species and the promotion of plant growth. Biol Control. 2021;152:104444. https://doi.org/10.1016/j.biocontrol.2020.104444.
33. Zhang HF, Wang N, Wang YC, Wang JJ, Zheng H, Liu ZH. Cloning and heterologous expression of SS10, a subtilisin-like protease

displaying antifungal activity from *Trichoderma harzianum*. Biocontrol Sci. 2017;22:145–52. https://doi.org/10.1111/j.1574-6968.2008.01403.x.
34. Wang R, Long ZY, Liang XY, Guo SL, Ning N, Yang LN, Wang X, Lu BH, Gao J. The role of a β-1,3–1,4-glucanase derived from Bacillus amyloliquefaciens FS6 in the protection of ginseng against Botrytis cinerea and Alternaria panax. Biol Control. 2021;164:104765. https://doi.org/10.1016/j.biocontrol.2021.104765.
35. Han JZ, Wang F, Gao P, Ma Z, Zhao SM, Lu ZX, Lv FX, Bie XM. Mechanism of action of AMP-jsa9, a LI-F-type antimicrobial peptide produced by *Paenibacillus polymyxa* JSa-9, against *Fusarium moniliforme*. Fungal Genet Biol. 2017;104:45–55. https://doi.org/10.1016/j.fgb.2017.05.002.
36. Wang R, Liang X, Long Z, Wang X, Yang L, Lu B, Gao J. An LCI-like protein APC2 protects ginseng root from *Fusarium solani* infection. J Appl Microbiol. 2021;130:165–78. https://doi.org/10.1111/jam.147717.
37. Natarajan K, Balasubramanian V, Kannan RV. Investigation of antifungal activity of surfactin against mycotoxigenic phytopathogenic fungus *Fusarium moniliforme* and its impact in seed germination and mycotoxicosis. Pestic Biochem Phys. 2019;155:101–7. https://doi.org/10.1016/j.pestbp.2019.01.010.
38. Laird M, Piccoli D, Weselowski B, McDowell T, Renaud J, MacDonald J, Yuan ZC. Surfactin-producing Bacillus velezensis 1B–23 and Bacillus sp 1D–12 protect tomato against bacterial canker caused by Clavibacter michiganensis subsp Michiganensis. J Plant Pathol. 2020;102:451–8. https://doi.org/10.1007/s42161-019-00461-w.
39. Mülner P, Schwarz E, Dietel K, Herfort S, Jähne J, Lasch P, Cernava T, Berg G, Vater J. Fusaricidins, polymyxins and volatiles produced by *Paenibacillus polymyxa* strains DSM 32871 and M1. Pathogens. 2021;10:1485. https://doi.org/10.3390/pathogens10111485.

Publisher's Note